

Accelerator modes in Stochastic Electron Heating

Alexey R. Knyazev

University of California, San Diego, CA 92093, USA

aknyazev@ucsd.edu

Abstract—Report discusses the role of accelerator modes in super diffusive transport on an example of Stochastic Electron acceleration. Physical model of electron acceleration by laser field in a longitudinal electrostatic trap is presented with the corresponding discrete map \mathfrak{E} . The GALI method of chaos detection is discussed and applied to reveal the structure of the \mathfrak{E} phase space. Momentum distribution of \mathfrak{E} is described with Levy stable distributions.

field along the laser wave propagation is added and discussed in section II-B. The discrete mapping approximating such system's dynamics is introduced.

A. Electron and plane wave envelope

This section discusses the interaction of a single electron with a plane wave and introduces notation for future reference. Consider the coordinate system where the electron is initially immobile and the wave vector $\mathbf{k} \parallel \mathbf{e}_x$. The EM wave structure can be described by a vector potential \mathbf{A} as follows:

$$\begin{aligned}\mathbf{B} &= \nabla \times \mathbf{A} \\ \mathbf{E} &= \nabla\phi - \frac{1}{c} \frac{\partial \mathbf{A}}{\partial t} \\ \mathbf{A} &= \frac{amc^2}{|e|} \mathbf{e}_y \\ a &= a_0 F(\xi) \sin(\xi)\end{aligned}$$

Where $\xi \equiv 2\pi(x - ct)/\lambda$ and $a_0 \equiv |e|E_0/mc\omega$.

According to the choice of \mathbf{A} above, electric field of the wave has non-zero component along y -axis only, magnetic field of the wave has non-zero component along z -axis only. The particle dynamics is then described by:

$$\begin{aligned}\frac{d}{dt} \left(\frac{p_x}{mc} \right) &= -\frac{v_y}{c} \frac{|e|B_z}{mc} \\ \frac{d}{dt} \left(\frac{p_y}{mc} \right) &= -\frac{|e|E_y}{mc} + \frac{v_x}{c} \frac{|e|B_z}{mc} \\ \frac{d}{dt} \left(\frac{p_z}{mc} \right) &= 0 \\ \mathbf{p} &= \gamma m \mathbf{v} \\ \gamma &= \sqrt{1 + p^2/m^2c^2}\end{aligned}$$

Expressed in terms of vector potential

$$\frac{|e|E_y}{mc} = \frac{|e|B_z}{mc} = \frac{|e|}{mc} \frac{2\pi}{\lambda} \frac{dA}{d\xi} = \omega \frac{da}{d\xi}$$

Second Newton's law above can be rewritten as

$$\begin{aligned}\frac{1}{\omega} \frac{d}{dt} \left(\frac{p}{mc} \right) &= -\frac{v_y}{c} \frac{da}{d\xi} \\ \frac{1}{\omega} \frac{d}{dt} \left(\frac{p_y}{mc} \right) &= \left(-1 + \frac{v_x}{c} \right) = \frac{1}{\omega} \frac{da}{d\xi} \frac{d\xi}{dt}\end{aligned}$$

Which reveals the integral of motion

$$\frac{d}{dt} \left(\frac{p_y}{mc} - a \right) = 0$$

Which for initially immobile electron gives

CONTENTS

I	Introduction:	1
II	Physical model	1
	II-A Electron and plane wave envelope . . .	1
	II-B Longitudinal electrostatic trap	2
III	Analysis	3
	III-A Chaos detection	3
	III-B α -stable distributions	3
	III-C About accelerator modes	5
IV	Simulations	5
	IV-A Calculating diffusion \mathcal{D}_{num}	5
	IV-B Calculating scaling exponent μ_{num} . . .	6
	References	6

I. INTRODUCTION:

UNDERSTANDING the super diffusion regime properties associated with accelerator modes can help increase the efficiency of stochastic electron heating. This project paper employs both classical and recent (see references) tools to better understand the role played by accelerator modes. Brief insight into the physical picture of a system exhibiting stochastic regimes is presented. The background on accelerator modes is provided and backed up with the simulation results.

II. PHYSICAL MODEL

This section discusses a simple setup for stochastic electron heating. It begins with discussing the interaction of electron with a plane electromagnetic wave. In section II-A, the interaction of electron with a plane wave envelope is considered, discussing the importance of dephasing rate δ (introduced below) for electron acceleration efficiency. Is is also shown that such setup does not allow electron to retain any of the laser pulse energy after the interaction. To overcome the restriction of the Lawson-Woodward theorem, the longitudinal electrostatic

$$p_y = amc$$

Another integral of motion is

$$\frac{d}{dt} \left(\gamma - \frac{p_x}{mc} \right) = 0$$

Which for initially immobile electron gives

$$\gamma = 1 - \frac{p_x}{mc}$$

From these two integrals of motion, the expression for longitudinal momentum is

$$\begin{aligned} \frac{1}{\omega} \frac{d}{dt} \left(\frac{p}{mc} \right) &= -\frac{v_y}{c} \frac{da}{d\xi} \\ \frac{p_x}{mc} &= \frac{a^2}{2} \end{aligned}$$

Expressions for p_x and p_y illustrate that the electron does not retain its energy after the electric pulse, (when $F(\xi) \rightarrow 0$ as $\xi \rightarrow \infty$). This is in agreement with the Lawson-Woodward theorem.

Acceleration of the particle is sensitive to initial condition, which can be seen from the derived integrals of motion

$$\begin{aligned} p_y - amc &= 0 \\ \gamma - p_x/mc &= \sqrt{1 + p_0^2/m^2c^2} - p_0/mc = I \\ \frac{p_x}{mc} &= \frac{a^2 + 1 - I^2}{2I} \end{aligned}$$

So for the non-relativistic electron $I \approx 1$, for relativistic with initial longitudinal momentum p_0 :

$$I = \sqrt{1 + p_0^2/m^2c^2} - p_0/mc \approx \frac{mc}{2p_0} \ll 1$$

and for $p_0 < 0$:

$$I = \sqrt{1 + p_0^2/m^2c^2} - p_0/mc \approx \frac{2|p_0|}{mc} \gg 1$$

Hence, pre-acceleration can greatly increase the interaction efficiency. The physical reason for it is the decrease in the dephasing rate between the electron and the wave,

B. Longitudinal electrostatic trap

One of the ways to retain energy from the laser-electron interaction is to trap the electron with an electrostatic field. Consider the laser pulse propagating through a longitudinal electrostatic potential well described by power law $U(z) = k_u|z|^p$. The dynamics of electron in this system can be described by a Hamiltonian (see ref.[2]).

$$H_z(z, \delta, \xi) = \frac{1}{2} \left(\frac{1 + (\hat{P}_x + A_x(\xi, z))^2}{\delta} + \delta \right) + U(z)$$

$$\begin{aligned} \frac{dz}{d\xi} &= -\frac{\partial H}{\partial \delta} \\ \frac{d\delta}{d\xi} &= -\frac{\partial H}{\partial z} \end{aligned}$$

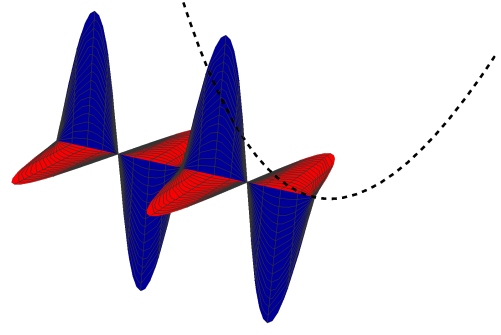


Fig. 1. Illustration of the setup described in section II-B. The laser (filled curve) propagates along the direction of longitudinal electrostatic trap, interacting with the electron. Confined by the trap (longitudinal potential well is depicted by black dashed line), electron oscillates and is able to enter the low dephasing rate regime (highly effective energy exchange) multiple times. This system can exhibit stochastic heating of the electron.

Note that the dephasing rate (the rate of change of laser wave phase in electron's frame of reference) $\delta = \gamma - p_z/mc$ is no longer constant. As was shown in the section II-A, low dephasing rate increases the efficiency of laser-electron acceleration. The dynamics of the electron in this system consists of almost adiabatic regions with periodic "kicks" in the low δ zones. (This is reminiscent of a kicked rotator corresponding to a Standard Map)

This is a 3/2 Hamiltonian which allows to employ the machinery developed for analysing chaos in a low-dimensional systems. In order to obtain the Poincare cross-section of the phase space, it is possible to integrate the dynamics of this system directly. To recover the cross-sections topology this way is however complicated. First, it requires exponentially long simulation times. Second, the integrator needs to respect the symplectic structure of the Hamiltonian system, and the only known schemes that respect this property are implicit, meaning one will be faced with solving stiff systems of non-linear algebraic equations which can introduce errors from the solver and imposes strict time resolution restrictions (adaptive time step methods also don't solve the resolution problem since such integrator's class only guarantees bounded relative error in energy, which in practice can reach orders of magnitude deviations for not conservative Hamiltonian systems). Third, even within the class of fixed step symplectic integrators the discretization itself can alter the stochastic properties of the calculated trajectories. Because of these reasons one wants to obtain a discrete Poincare cross section map analytically and study its properties instead of direct integration.

It was shown that such cross section for the dynamics of laser-electron interaction in a longitudinal electrostatic trap within the appropriate asymptotics can be approximated by a discrete map \mathfrak{E} , similar to a Standard Map:

$$\begin{aligned} \Pi_{n+1} &= \Pi_n + Q \sin(\psi_n) \\ \psi_{n+1} &= \psi_n + \Pi_{n+1}^{1/2p-1} \end{aligned}$$

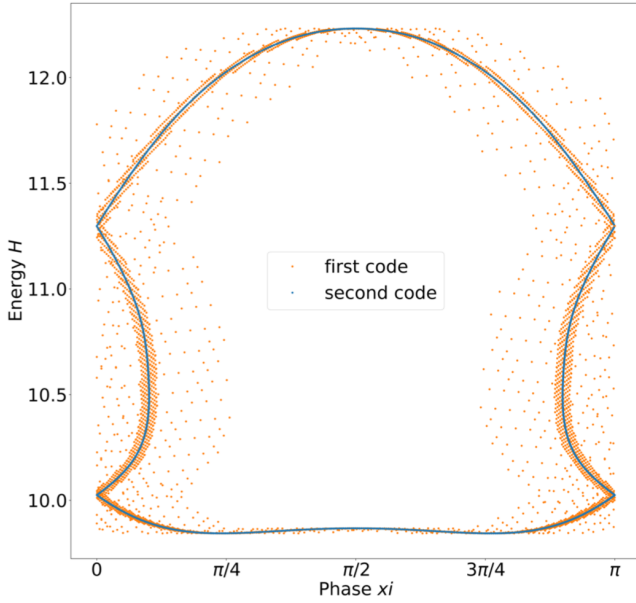


Fig. 2. Example of alternation of stochastic properties due to the integration scheme. Both integration schemes are symplectic (both are of SPRK class, code 1 corresponds to trapezoidal method and code 2 is a 4th order variational integrator), and both use the same nonlinear Broyden solver. Despite that, it is visible that the trapezoidal integrator does not recover the regular surface, and that significantly alters the resulting calculated Poincare cross-section.

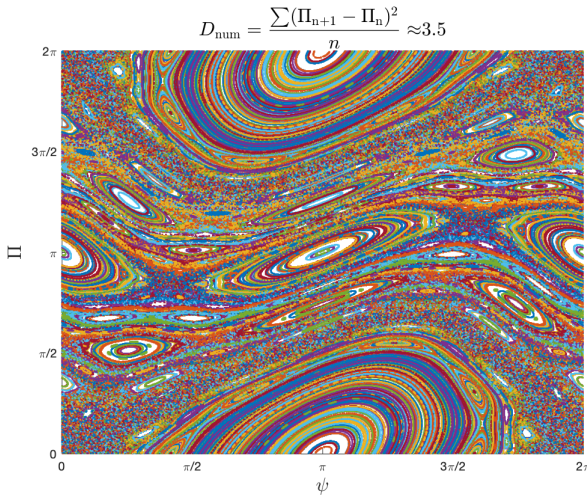


Fig. 3. Example of the phase space described by a map. Here $Q = 1$.

III. ANALYSIS

A. Chaos detection

Consider a discrete symplectic map \mathfrak{F} , describing the evolution of a conservative dynamical system over discrete times $t = n \in \mathbb{N}$. The phase space vector sequence \mathbf{x} and the corresponding deviation vector sequence are then given by recursive expressions:

$$\begin{aligned}\mathbf{x}_{n+1} &= \mathfrak{F}(\mathbf{x}_n) \\ \mathbf{w}_{n+1} &= \frac{\partial \mathfrak{F}}{\partial \mathbf{x}}(\mathbf{x}_n) \cdot \mathbf{w}_n\end{aligned}$$

Def. For a map \mathfrak{F} with N dimensions, the General Alignment Index of Order k (denoted GALI_k) is defined as the volume of the k -parallelogram:

$$\text{GALI}_k = \left\| \frac{\mathbf{w}_1}{\|\mathbf{w}_1\|} \wedge \frac{\mathbf{w}_2}{\|\mathbf{w}_2\|} \wedge \dots \wedge \frac{\mathbf{w}_k}{\|\mathbf{w}_k\|} \right\|$$

Where the order k is in range between 1 and N .

Map \mathfrak{E} is 2-dimensional, therefore GALI_2 is appropriate. In practise, GALI_2 is calculated as follows: First, a random unit vector is chosen associated with the initial condition \mathbf{x}_1 . This is the first deviation vector \mathbf{w}_1 . The second deviation vector \mathbf{w}_2 is chosen to be orthogonal to \mathbf{w}_1 . According to definition, the GALI_2 index is then simply

$$\text{GALI}_2 = \det \begin{pmatrix} w_{11} & w_{11} \\ w_{21} & w_{21} \end{pmatrix}^{1/2}$$

The values of the deviation vectors are then updated and renormalized to unity, and the process repeats. Conservation of phase volume by Hamiltonian system (described by \mathfrak{E}) guarantees us that the Lyapunov exponents will have different signs $\lambda_1 = -\lambda_2 > 0$. In case of chaotic orbit the GALI_2 decays exponentially (the deviation vectors get stretched along the eigenvector of $\partial \mathfrak{F} / \partial \mathbf{x}$ that corresponds to positive Lyapunov exponent, therefore aligning and decreasing the associated parallelogram area.), meanwhile for a regular orbit of 2d system GALI_2 decays as a power law (deviation vectors collapse to the tangent surface of a torus which in 2d is 1-dimensional, hence also decreasing the associated parallelogram area but at a much slower rate). This provides a classification scheme of calculating the GALI_2 for fixed number of steps and evaluating if its value falls below the pre-defined classification threshold.

B. α -stable distributions

This section discusses the concept of Levy stable (α -stable) distributions and their relevance to stochastic dynamics. Notion of distribution's stability is motivated by the central limit theorem and it's generalizations. According to CLT, the sum of mutually independent normally distributed random variables is a normally distributed random variable, hence the probability distribution law is preserved for such linear combinations. Such property is denoted with $\stackrel{d}{=}$ symbol.

Def.1. Let $a, b, c \in \mathbb{R}^+$, and ξ_1, ξ_2 be independent random variables with same probability distribution \mathbb{P} . If random variable

$$\xi \stackrel{d}{=} a\xi_1 + b\xi_2 + c,$$

also has probability distribution \mathbb{P} , then \mathbb{P} is called stable distribution. Examples of stable probability distributions with a closed form are Gaussian, Cauchy and Levy distributions. The tails of the stable distribution are can be "fat", i.e. governed by the power law behavior. While providing intuitive

Fig. 4. Examples of how $GALI_2$ depends on number of iterations n for trajectories of varying degree of stochasticity. Phase trajectories labeled a, b, c correspond to plots b, d, f , respectively. The value of $GALI_2$ after 50 iterations is a significant classification feature for determining if the trajectory is chaotic (and can also be used as a measure of stochasticity).

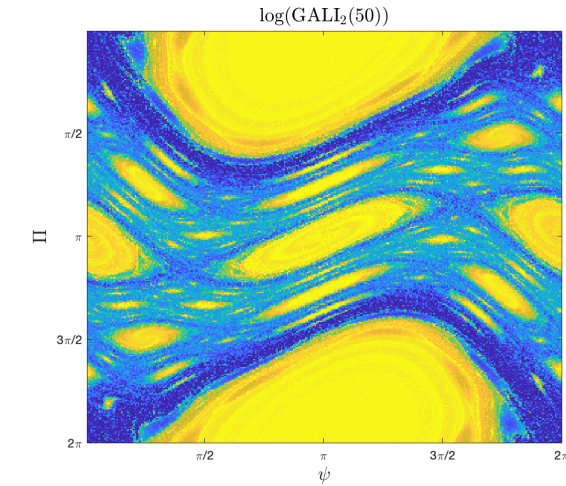
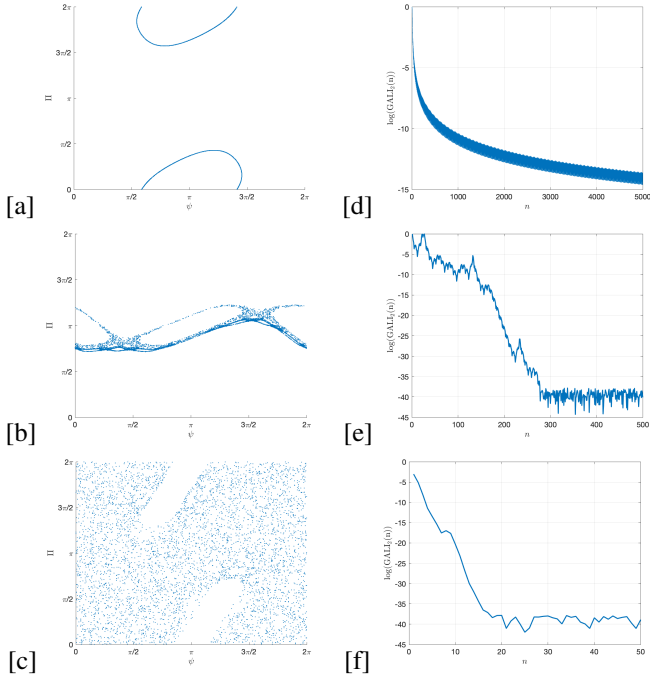


Fig. 5. Example of the $GALI_2$ plot. Here $Q = 1$.

understanding of the concept, the Def.1 has a disadvantage of not providing any systematic way of parametrizing the entire class of stable distributions. Equivalent definition of stability solves this problem:

Def.2. Random variable ξ is called stable if $\xi \stackrel{d}{=} a\xi_1 + b$, where ξ_1 is a random variable with distribution function $F_{\xi_1}(x)$ and characteristic function:

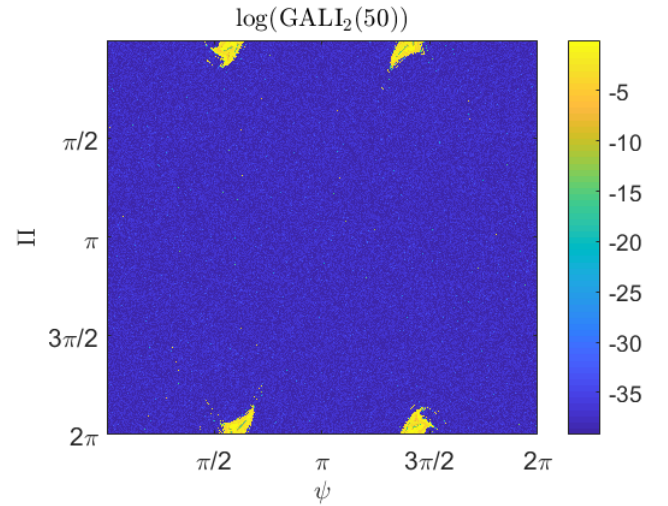


Fig. 6. $GALI_2$ plot for $Q = 6.6$, corresponding to the first spike on the fig. 10. Islands correspond to the accelerator modes. Magnification of the island is shown at fig. 7

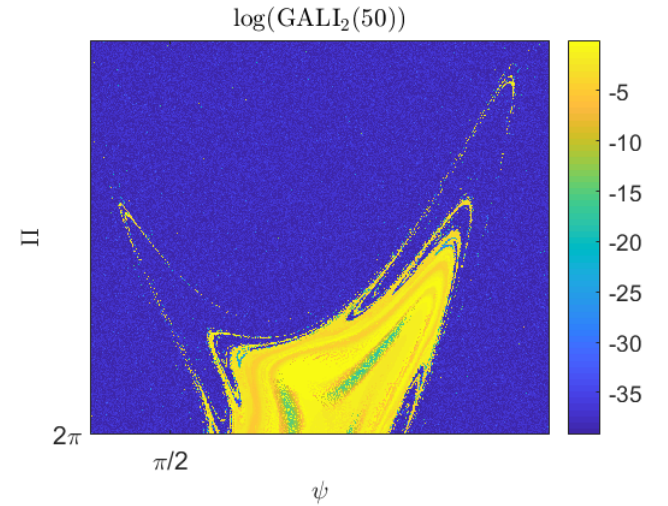


Fig. 7. Magnification of one of the islands from fig. 6

$$\int_{-\infty}^{\infty} \exp(iux) dF_{\xi_1}(x) = \begin{cases} \exp(-|u|^\alpha (1 - i\beta \tan \frac{\pi\alpha}{2}(\frac{u}{|u|}))) & \alpha \neq 1 \\ \exp(-|u|(1 + i\beta \frac{2}{\pi}(\frac{u}{|u|}) \log |u|)) & \alpha = 1 \end{cases},$$

where $\alpha \in (0, 2]$ is the characteristic exponent (also called index of stability), $\beta \in [-1, 1]$ is the skewness parameter, $a \neq 0$ is a scale parameter (also denoted γ) and, $b \in \mathbb{R}$ is the location parameter (also denoted δ). Several parameterizations are used for describing stable distributions (different ones denoted by values of $k = 0, 1, \dots$); in simulations here the so-called zero type ($k = 0$) parameterization is used, corresponding to random variables ξ given by

$$\xi \stackrel{d}{=} \begin{cases} \gamma(\xi_1 - \beta \tan(\frac{\pi\alpha}{2})) + \delta \alpha \neq 1 \\ \gamma\xi_1 + \delta \alpha = 1 \end{cases},$$

has characteristic function

$$S(\alpha, \beta, \gamma, \delta; 0) = \begin{cases} \exp(iu\delta - \gamma^\alpha |u|^\alpha (1 + i\beta(-1 + |u\gamma|^{1-\alpha} \tan(\frac{\pi\alpha}{2})))) \alpha \neq 1 \\ \exp(iu\delta - \frac{\gamma|u|(\pi + 2i\beta \log(|u\gamma|)(u))}{\pi}) \alpha = 1 \end{cases}$$

C. About accelerator modes

This section discusses the concept of accelerator modes on an example of a standard map (\mathfrak{S} for the case $p = 1$):

$$\begin{aligned} \Pi_{n+1} &= \Pi_n + Q \sin(\psi_n) \\ \psi_{n+1} &= \psi_n + \Pi \end{aligned}$$

Such map permits ballistic propagation along Π and/or ψ directions if

$$Q \sin(\psi_0^a) = 2\pi l \Pi_0^a = 2\pi m,$$

where m and l are integers. In such case,

$$p_n^a = 2\pi l n + p_0^a$$

is called the accelerator mode. It is evident that it corresponds to ballistic transport since $\Pi \propto n$ and $\psi \propto n^2$. The linear stability region of the accelerator mode can be found by a standard procedure of finding the eigenvalues of the associated with the map \mathfrak{S} Jacobian matrix (tangent map $\partial\mathfrak{S}/\partial\mathbf{x}$). For Standard Map the Jacobian matrix is

$$\begin{vmatrix} 1 & Q \cos(\psi) \\ 1 & 1 + Q \cos(\psi) \end{vmatrix}$$

and the corresponding characteristic equation is

$$\lambda^2 - 2\lambda \left(1 + \frac{1}{2}Q \cos(\psi)\right) + 1 = 0.$$

The eigenvalues $\lambda_{1,2}$ are given by

$$\lambda = 1 + \frac{1}{2}Q \cos(\psi) \pm \left(\left(1 + \frac{1}{2}Q \cos(\psi)\right)^2 - 1 \right)^{1/2}$$

Linearly stable region $\text{Re}(\lambda_{1,2}) < 0$ corresponds to

$$-2 > Q \cos \psi > -4$$

so the accelerator mode is stable for

$$2\pi l < Q < [4 + (2\pi l)^2]^{1/2}$$

Classical example of the Standard Maps' phase space with $Q = 6.28 \approx 2\pi$ is shown on fig. 8.

The ballistic trajectories of the accelerator mode correspond to the regular surfaces inside the island visible on fig. 9. Due to the stickiness of the island, the surrounding trajectories are

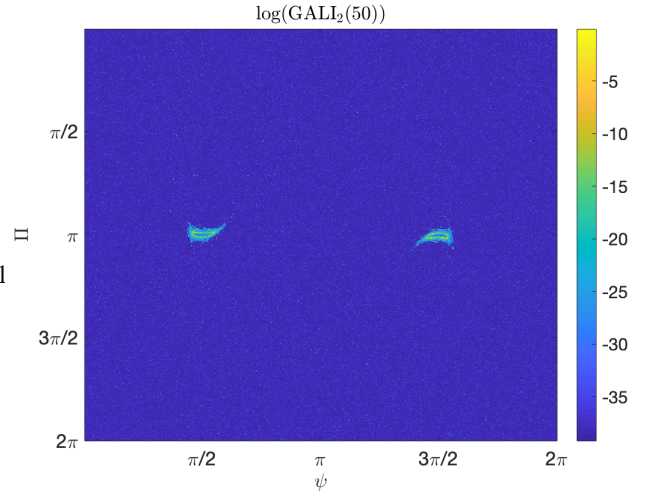


Fig. 8. $\text{GALI}_2(50)$ plot for $Q = 6.28 \approx 2\pi$. Islands correspond to acceleration mode. See magnification of the island on fig. 9

dragged along by accelerator modes trajectories, and therefore affecting their transport. Such interpretation can be verified directly by calculating the dependence of the scaling exponent μ_{num} (See section IV-B for more details) on the initial conditions $[\Pi_0, \Psi_0]$. As the order l of the accelerator mode increases, the region of stability shrinks and the associated phase space islands become smaller.

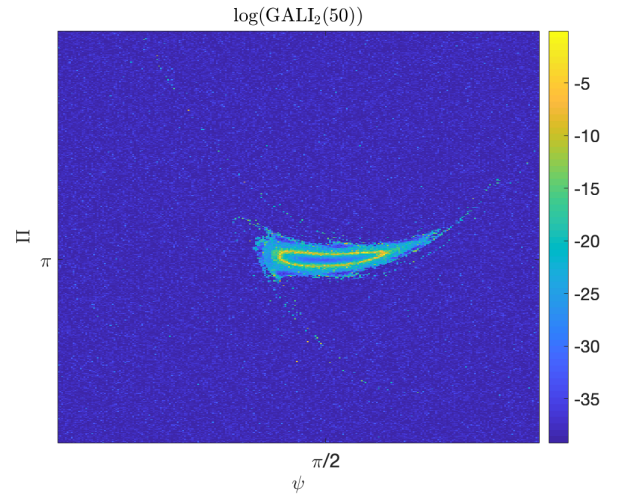


Fig. 9. $\text{GALI}_2(50)$ plot for $Q = 6.28 \approx 2\pi$. Islands correspond to acceleration mode.

IV. SIMULATIONS

A. Calculating diffusion \mathcal{D}_{num}

The numerically simulated coefficient of diffusion was defined as

$$\mathcal{D}_{\text{num}} = \frac{\langle (\Delta\Pi)^2 \rangle}{n}$$

where the $\langle \dots \rangle$ brackets denote the ensemble average (averaging was conducted over 314^2 evenly distributed initial conditions $(\Pi, \psi) \in [0, 2\pi] \times [0, 2\pi]$). The calculated dependence of $\mathcal{D}_{\text{num}}/(Q^2)$ for three different iteration numbers n is presented on a figure. The quasilinear approximation for a Diffusion coefficient of a Standard Map yields $\mathcal{D}_{\text{QL}} = K^2/2$, however for superdiffusive case $\langle (\Delta\Pi)^2 \rangle \propto t^\mu$, where $\mu \in [0, 2]$. The case of $\mu = 2$ is associated with accelerator modes and corresponds to the case of ballistic transport.

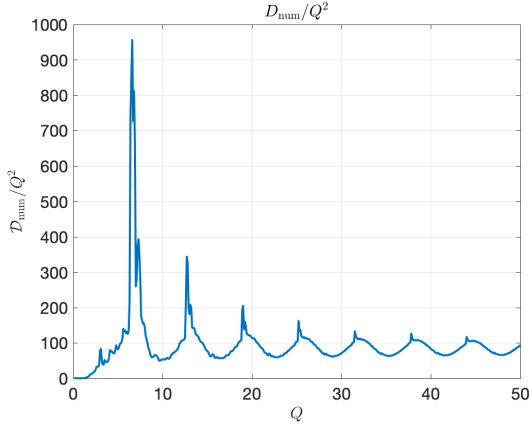


Fig. 10. Calculated values of $\mathcal{D}_{\text{num}}/(Q^2)$ for $n = 1000$ iterations. The increments across Q -axis $\delta Q = 0.1$. The values of Q corresponding to peaks are listed in the table I

TABLE I

Q VALUES ASSOCIATED WITH ACCELERATOR MODES, SEE FIG. 10

Q	α	β	γ	δ
6.6	-	-	-	-
12.7	-	-	-	-
19	-	-	-	-
25.2	-	-	-	-
31.5	-	-	-	-
37.8	-	-	-	-
44	-	-	-	-

B. Calculating scaling exponent μ_{num}

The scaling exponent μ can be obtained from fitting the $\log\langle(\Delta\Pi)^2\rangle$ on $\log(n)$ dependence. Comparison between two types of diffusion, $Q = 6.6$ associated with accelerator mode and $Q = 10$ as a reference case with a fully chaotic space is shown on fig. 11.

REFERENCES

- [1] M. M. Murnane, H. C. Kapteyn, S. P. Gordon, J. Bokor, E. N. Glytsis, and R. W. Falcone. Accelerator modes and their effect in the diffusion properties in the kicked rotator. 2017
- [2] Yanzeng Zhang, S.I. Krashennnikov and Alexey Knyazev. Stochastic electron heating in the laser and quasi-static electric and magnetic fields. 2018
- [3] DISCRETE HAMILTONIAN VARIATIONAL INTEGRATORS, 2010
- [4] A. V. Arefiev, A. P. L. Robinson and V. N. Khudik. Novel aspects of direct laser acceleration of relativistic electrons, 2015
- [5] G.M. Zaslavsky. Chaos, fractional kinetics, and anomalous transport, 2002
- [6] G.M. Zaslavsky Hamiltonian Chaos Fractional Dynamics, 2005
- [7] Chirikov Universal Instabilities of many dimensional systems
- [8] Shiryayev. Probability-2, 2015
- [9] John P. Nolan. Stable Distributions, Models for Heavy Tailed Data, 2018

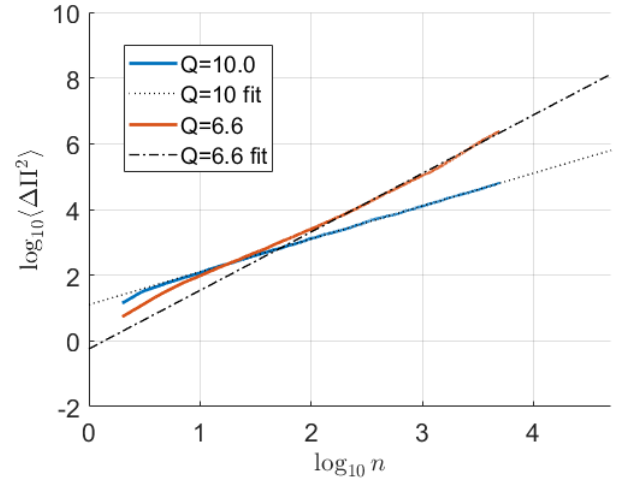


Fig. 11. This picture illustrates the technique of measuring the scaling exponent μ_{num} . One can calculate the evolution of the $\langle(\Delta\Pi)^2\rangle$ (here $\langle \dots \rangle$ corresponds to averaging over ensemble of initial conditions. For this calculation, the ensemble of 314^2 evenly distributed initial conditions $[\Pi, \psi] = [0, 2\pi] \times [0, 2\pi]$ was used) and fits it to exponential law $\langle(\Delta\Pi)^2\rangle \propto n^\mu$ by linearly fitting the log-graph, hence obtaining the polynomial coefficient $\mu_{\text{num}} \log(n)$. For example $Q = 10.0$ correspond to fully chaotic regime and exhibits normal diffusion scaling with $\mu_{\text{num}} \approx 1.0$, and $Q = 6.6$ (max of fig. 10 associated with accelerator mode) exhibits superdiffusion with $\mu_{\text{num}} \approx 1.78$

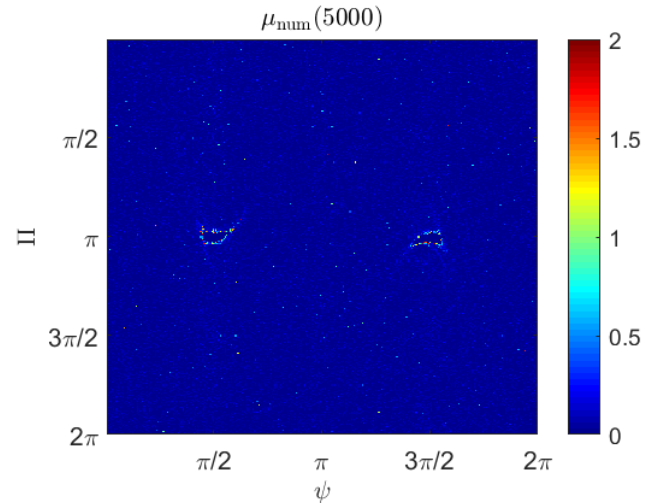


Fig. 12. Map showing dependence of $\mu_{\text{num}}(5000)$ on initial conditions for $Q = 6.28$